UNIVERSITY OF LEEDS

This is a repository copy of *Feedhorn-integrated THz QCL local oscillators for the LOCUS atmospheric sounder*.

White Rose Research Online URL for this paper:
http://eprints.whiterose.ac.uk/102549/

Version: Accepted Version

Proceedings Paper:

eprints@whiterose.ac.uk
https://eprints.whiterose.ac.uk/

Feedhorn-integrated THz QCL local oscillators for the LOCUS atmospheric sounder

A. Valavanis*, M. Henry†, Y. Han*, O. Auriacombe†, R. Dong*, T. Rawlings†, L. H. Li*, M. Oldfield†, N. Brewster†, A. G. Davies*, B. N. Ellison†, and E. H. Linfield*

*School of Electronic and Electrical Engineering, University of Leeds, Leeds LS2 9JT, U.K.,
Email: a.valavanis@leeds.ac.uk
†STFC Rutherford Appleton Laboratory, Harwell Oxford, Didcot OX11 0QX, U.K.

Abstract—The LOCUS atmospheric sounder is a satellite-borne THz radiometer concept, for studying molecular species in the mesosphere and lower thermosphere. We report waveguide-integrated THz quantum-cascade lasers for use as 3.5 THz local oscillators. A waveguide-integration scheme, using an integrated diagonal feedhorn significantly improves power outcoupling. 1.3 mW THz emission is demonstrated in a space-qualified Stirling cryocooler at 57 K, with ∼15° beam divergence.

I. INTRODUCTION AND BACKGROUND

THE Mesosphere and Lower Thermosphere (MLT) of the Earth's atmosphere represents a "gateway" between the lower atmosphere and the near-space environment. Its temperature response to greenhouse gases and ozone depletion is significantly stronger than that of the troposphere and as such is an extremely sensitive climate change indicator [1]. However, mapping of key MLT species (O, OH, CO and NO) has not been achieved, owing to a lack of satellite instrumentation capable of resolving spectral lines in the 1–5 THz band. We present optimised 3.5 THz local oscillators (LOs), based on quantum-cascade lasers (QCLs) for the LOCUS limb sounder instrument (Linking Observations of Climate, the Upper Atmosphere and Space-weather) —a satellite-based THz radiometer concept. A waveguide-integration scheme improves the robustness, and performance of the QCLs while reducing the need for external optics. A recently-developed integration approach [2], based on a bound-to-continuum (BTC) QCL and a rectangular waveguide yielded good thermal and electronic performance but relatively poor power outcoupling. Here, we significantly improve the outcoupling and beam profile by using a higher performance phonon-assisted QCL design and an integrated feedhorn.

II. DEVICE FABRICATION

A 9-well hybrid QCL active region [3] was chosen, owing to its high THz output power and operating temperature range. The design was adapted for emission frequency at 3.5 THz and the resulting $GaAs/Al_{0.15}Ga_{0.85}As$ heterostructure was grown using molecular-beam epitaxy on a semi-insulating GaAs substrate. A section of the wafer was processed into an array of 13 parallel Au–Au ridge-waveguides [4] with 125 μm width, and cleaved to a length of 980 μm.
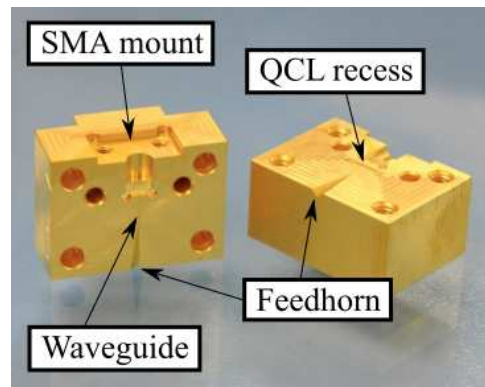

Fig. 1. Micromachined 3.5-THz QCL waveguide block assembly, with the diagonal feedhorn, rectangular waveguide, mounting-point for an electrical SMA connector and the QCL-mounting recess indicated. In the completed assembly, the two half-blocks are co-registered to form the waveguide and feedhorn structures.

Two halves of an overmoded $300 \times 150\,\mu m^2$ rectangular waveguide, terminated with a diagonal feedhorn, were machined into a pair of copper blocks, as shown in Fig. 1. The QCL array was indium-soldered into a recess at the rear of one of the blocks, with the facet of the central QCL aligned with the waveguide channel. The other lasers in the array were unused. Electrical bias was supplied through a gold ribbon bond, attached to an integrated SMA connector, and additional ribbon bonds were connected to the unused laser ridges for mechanical stability. The two half-blocks were co-registered to enclose the QCL and form the completed rectangular waveguide and diagonal feedhorn assemblies.

A second QCL device was processed from the same wafer, using a 60 μm ridge width, and a reduced substrate thickness of 100 μm. The QCL was diced into a standalone 100 μm-wide chip. The reduced device dimensions, compared with the array described above, enable its direct integration into the waveguide channel as opposed to a separate recess, and hence potentially improve the optical coupling efficiency.

III. PERFORMANCE CHARACTERIZATION

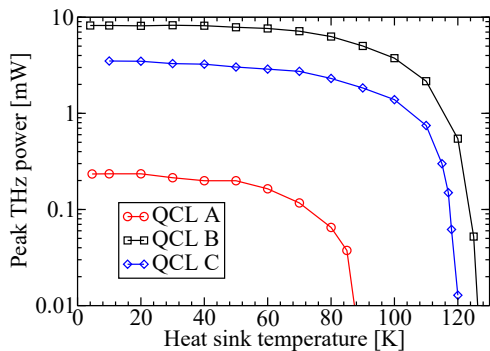Initial device characterisation was undertaken in a continuous-flow Janis ST-100 helium crysotat. A pulsed drive

Fig. 2. Peak pulsed THz power, showing results for 'A' the rectangular-waveguide system described in in [2], 'B' the new feedhorn-integrated system, and 'C' the reduced-dimension device mounted directly into the waveguide

Fig. 3. Terahertz power transmitted from QCL block 'B' through a polarizer as a function of angle

current was supplied (10-kHz, 2%-duty-cycle) using an Agilent 8114A pulse-generator, which was gated by a 167-Hz modulation envelope. The emitted THz radiation was collimated and focused into a helium-cooled Ge:Ga photoconductive detector using a pair of off-axis paraboloidal mirrors and the time-averaged detector signal was recorded using a lock-in amplifier. The THz output power was measured as a function of temperature, with the detector output being calibrated using a photoacoustic power meter. Fig. 2 shows that the feedhorn-integrated block offers significantly improved performance over that obtained using a simple rectangular waveguide, as reported in Ref. [2]. Maximum (pulsed) operating temperature and output power raised to 127 K and 8.2 mW respectively (c.f., 88 K and 0.2 mW previously). The single QCL device, mounted directly into the waveguide channel (device 'C' in Fig. 2), yielded a lower output power of 3.4 mW owing to its reduced active region dimensions. The operating temperature range was, however, reduced by only 7 K.

Continuous-wave (cw) operation of Block 'B' was demonstrated within a space-qualified Stirling-cycle cryocooler (heat-lift ∼5 W), with 1.3 mW THz power being emitted at a steady-state heat-sink temperature of 57 K. The far-field beam-profile was measured by scanning a Golay detector at a distance of ∼57 mm outside the cryocooler. The beam waist was found to have ∼15° divergence, which represents an improvement over the 20° previously reported for Block 'A' [2]).

The THz beam polarization was measured by rotating a pair of wire-grid polarizers in the beam axis and recording the transmitted THz power. Fig. 3 shows that a significant proportion of the radiation was transmitted through the anti-aligned polarizer, indicating an elliptically polarized beam. A Jones calculus model of the system, accounting for the isotropic absorption and leakage factor of the non-ideal polarizers, was used to determine the polarization ellipticity $R = 1.34$. By contrast, an identical QCL mounted on a simple copper heat-sink block was found to be linearly polarized.

IV. CONCLUSION

Integrated 3.5 THz local-oscillator blocks, consisting of a QCL, waveguide, feedhorn, temperature sensor and bias con-
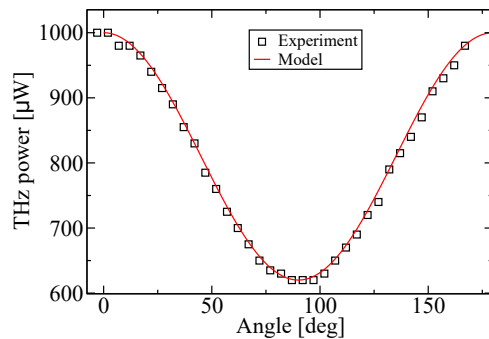
nector has been demonstrated in a space-qualified cryocooler. These devices yield upto a factor of 40 improvement in output power, compared with our previously reported results, and operate up to 120 K (pulsed) or 80 K continuous-wave. By reducing the dimensions of the QCL, it was possible to integrate the device directly into the waveguide channel. Although this approach reduces the total output power from the device, the coupling efficiency is potentially improved, and the reduced heat dissipation will assist integration with compact cryocoolers. Our measurements indicate that the block integration approach introduces a shift in the polarization state of the device, and this phenomenon will be analyzed further in our subsequent work. This device construction approach will underpin our development of fully-integrated THz systems for satellite and laboratory applications.

REFERENCES

[1] G. Beig, P. Keckhut, R. P. Lowe, R. G. Roble, M. G. Mlynczak, J. Scheer, V. I. Fomichev, D. Offermann, W. J. R. French, M. G. Shepherd, A. I. Semenov, E. E. Remsberg, C. Y. She, F. J. Lbken, J. Bremer, B. R. Clemesha, J. Stegman, F. Sigernes, and S. Fadnavis, "Review of mesospheric temperature trends," *Rev. Geophys.*, vol. 41, no. 4, p. 1015, Dec. 2003. [Online]. Available: http://0-onlinelibrary.wiley.com.wam.leeds.ac.uk/doi/10.1029/2002RG000121/abstract

[2] A. Valavanis, J. Zhu, N. Brewster, L. Li, R. Dong, Y. Han, E. Linfield, M. Oldfield, P. Dean, B. Ellison, A. Davies, and L. Bushnell, "Mechanically robust waveguide-integration and beam shaping of terahertz quantum cascade lasers," *Electron. Lett.*, vol. 51, no. 12, pp. 919–921, Jun. 2015. [Online]. Available: http://digital-library.theiet.org/content/journals/10.1049/el.2015.1137

[3] M. Wienold, L. Schrottke, M. Giehler, R. Hey, W. Anders, and H. Grahn, "Low-voltage terahertz quantum-cascade lasers based on LO-phonon-assisted interminiband transitions," *Electron. Lett.*, vol. 45, no. 20, pp. 1030–1031, Sep. 2009.

[4] B. S. Williams, S. Kumar, H. Callebaut, Q. Hu, and J. L. Reno, "Terahertz quantum-cascade laser at 100 m using metal waveguide for mode confinement," *Applied Physics Letters*, vol. 83, no. 11, pp. 2124–2126, Sep. 2003. [Online]. Available: http://0-scitation.aip.org.wam.leeds.ac.uk/content/aip/journal/apl/83/11/10.1063/1.1611642